






Oceanic Mesoscale Cyclones Cluster Surface Lagrangian Material

Clément Vic¹ , Solenne Hascoët¹ , Jonathan Gula^{1,2} , Thierry Huck¹ , and Christophe Maes¹ 

¹Laboratoire d'Océanographie Physique et Spatiale, University of Brest, CNRS, IRD, Ifremer, Plouzané, France, ²Institut Universitaire de France (IUF), Paris, France

Key Points:

- Surface Velocity Program drifters are preferentially trapped into mesoscale cyclones rather than in anticyclones
- Lagrangian analysis of a mesoscale-resolving simulation shows that particles cluster preferentially in cyclonic fronts and eddies
- Particles cluster in cyclonic regions a few days before the formation and detection of mesoscale cyclones

Supporting Information:

Supporting Information may be found in the online version of this article.

Correspondence to:

C. Vic,
clement.vic@ifremer.fr

Citation:

Vic, C., Hascoët, S., Gula, J., Huck, T., & Maes, C. (2022). Oceanic mesoscale cyclones cluster surface Lagrangian material. *Geophysical Research Letters*, 49, e2021GL097488. <https://doi.org/10.1029/2021GL097488>

Received 16 DEC 2021
Accepted 3 FEB 2022

Author Contributions:

Conceptualization: Clément Vic, Jonathan Gula, Thierry Huck, Christophe Maes

Data curation: Clément Vic, Solenne Hascoët

Formal analysis: Clément Vic, Solenne Hascoët

Investigation: Clément Vic, Solenne Hascoët

Methodology: Clément Vic, Solenne Hascoët, Jonathan Gula, Thierry Huck, Christophe Maes

Software: Solenne Hascoët, Jonathan Gula

Supervision: Clément Vic, Jonathan Gula, Thierry Huck, Christophe Maes

Writing – original draft: Clément Vic
Writing – review & editing: Solenne Hascoët, Jonathan Gula, Thierry Huck, Christophe Maes

Abstract An asymmetry in the clustering of oceanic surface material has been observed at the submesoscales. Energetic and ephemeral submesoscale cyclonic fronts are associated with convergence zones, hence cluster surface material. Their anticyclonic counterparts do not feature such an effect. Yet, at the mesoscale, literature has been contradictory about such an asymmetry. Here, we combine surface drifter trajectories with an altimetry-derived mesoscale eddy database in the North Atlantic to show that mesoscale cyclones contain 24% more drifters than anticyclones. A numerical Lagrangian experiment using a mesoscale-resolving model quantitatively reproduces the observational results. It reveals that particles preferentially cluster in cyclonic regions, both in fronts and eddies. The model further suggests that ageostrophic cyclonic fronts concentrate particles a few days before the eddy formation and detection.

Plain Language Summary Earth's oceans are filled with swirling coherent structures called eddies, whose dominant scales range from 10 to 100 km across. Clockwise-rotating and counter-clockwise-rotating eddies, called anticyclones and cyclones in the northern hemisphere, coexist in the oceans with similar proportions and covered areas. Dominant theories for the life cycle of the largest eddies (mesoscale eddies) have concurred on their kinematic symmetry. However, this symmetry breaks down at the small scales (submesoscale eddies and fronts) and cyclonic structures have been shown to be associated with convergence zones. Here, we combined a surface drifter database with a satellite-derived mesoscale eddy database to show that mesoscale cyclones contain significantly more drifters than anticyclones. The use of a numerical Lagrangian experiment, that is, flow-following inert particles, unveiled that the clustering of particles occurs in the formation stage of the cyclones. This work has implications for our global understanding of the transport of surface material in the oceans, for example, debris and plastics.

1. Introduction

Mesoscale eddies are ubiquitous features in the oceans and dominate the kinetic energy reservoir. They mostly arise from instabilities of large-scale persistent currents and have been routinely observed through satellite altimetry for almost three decades (Chelton et al., 2011). They play an active role in the transport of tracers, yet several questions on the underlying mechanisms of dispersion and their regional and global implications remain debated (e.g., Abernathey & Haller, 2018; Zhang et al., 2014).

As put forward in McWilliams (2008), “almost all our understanding of eddy dynamics and phenomena has its roots in quasi-geostrophic theory”. Indeed, the dominant instabilities of large-scale currents and the lifecycle of mesoscale eddies are well described by the quasi-geostrophic theory. This theory relies on several assumptions, a fundamental one being that the Rossby number of the flow (Ro), which compares the inertial force to the Coriolis force, is small ($Ro < 0.1$, e.g., Section 5.3 in Vallis, 2006). In the limit of $Ro \rightarrow 0$, there is a perfect symmetry in the phenomenology of cyclones and anticyclones. For $Ro = O(0.1)$, an asymmetry is observed to develop with a dominance of anticyclones over cyclones. Correspondingly, the probability density function of the relative vorticity of the flow is slightly skewed toward negative values (e.g., Polvani et al., 1994). Reasons for this dominance are manifold (see the discussion in Polvani et al., 1994), but the sole kinematic consequence of the emergence of inertial forces is the acceleration of anticyclones and the slowing down of cyclones (Penven et al., 2014). No further kinematic asymmetry emerges from the regime of $Ro = O(0.1)$.

Two mechanisms commonly invoked to explain asymmetrical effects in convergence and divergence in cyclones and anticyclones are *eddy pumping* and *Ekman pumping* (McGillicuddy, 2016). The former is active toward the beginning and the end of the eddy life cycle (e.g., Figure 4.21 in Flierl & McGillicuddy, 2002). When a

surface-intensified eddy forms, isopycnals in the thermocline are pumped up (down) in cyclones (anticyclones), hence resulting in a divergence (convergence) of surface horizontal velocity in cyclones (anticyclones). The opposite happens when the eddy decays. The second mechanism – Ekman pumping (Gaube et al., 2015) – results from a differential wind stress on the upwind and downwind sides of the eddy, which creates a horizontal convergence (divergence) of Ekman transport in cyclones (anticyclones).

The oceanic surface boundary layer is host to a submesoscale regime of turbulence, where Ro reaches $O(1)$ values and the quasi-geostrophic regime does not hold. In this regime, vorticity is skewed toward positive values, and a clear dominance of cyclonic eddies and fronts has been observed and modeled (Buckingham et al., 2016; Rouillet & Klein, 2010; Rudnick, 2001; Shcherbina et al., 2013). There is growing evidence in the literature that submesoscale cyclonic vorticity is associated with convergence zones, both from Eulerian (Shcherbina et al., 2013) and Lagrangian observations (D'Asaro et al., 2018; Esposito et al., 2021). Theory and numerical modeling corroborate these observations (Barkan et al., 2019; Balwada et al., 2021).

We now elaborate on the Lagrangian implications of the mesoscale and submesoscale regimes of turbulence. If the mesoscale eddy field is ruled by a quasi-geostrophic regime, there should be an equipartition of Lagrangian material into mesoscale cyclones and anticyclones, stemming from their kinematic symmetry. However, it is tempting to extrapolate on the efficiency of submesoscale cyclonic flows to cluster material to test the hypothesis that an upscaling effect – compatible with an inverse cascade of turbulence in surface quasi-geostrophic flows (Capet et al., 2008) – could lead to a preferred accumulation of Lagrangian material into mesoscale cyclones. Submesoscales are ephemeral and difficult to observe but mesoscale eddies are easily tracked by satellite altimetry, so a potential asymmetry between the trapping capacity of cyclones and anticyclones could help to refine our understanding of the transport of surface passive tracers.

In this study, we focus on the North Atlantic Ocean between the equator and 45°N to encompass the equatorial and the subtropical gyre dynamics. We combine drifter data and a mesoscale eddy database to show that drifters are preferentially trapped into mesoscale cyclones compared to anticyclones. Those data sets limited any further investigation so we set up a Lagrangian numerical simulation to investigate the underlying mechanisms leading to this asymmetry. The article is organized as follows. Section 2 introduces the data sets and numerical framework used in this study. In Section 3, we present the observational and modeling results and in Section 4 we discuss and summarize them.

2. Data and Methods

2.1. Observations

We used the global daily mesoscale ocean eddy data set of Faghmous et al. (2015). An automatic eddy identification algorithm was used on AVISO's "Delayed Time," "all sat merged" global daily mean sea level anomalies on a 0.25° grid from January 1993 to May 2014. The data set consists in daily anticyclone and cyclone coordinates along with some properties, among which we only used the area.

We also used a subset of the Global Drifter Program (Lumpkin & Pazos, 2007; Niiler, 2001) data in the North Atlantic Ocean in the same time window as the eddy database. We selected a subset of drifters in 0° – 45°N and 110°W – 20°E , and then masked the data in the Pacific Ocean and the Mediterranean Sea. We retained only drogued drifters to discard trajectories that are too much influenced by wind effects (Grotsky et al., 2011; Poulain et al., 2009) and inertia (Beron-Vera et al., 2016). The data set gives 6 hr drifters' position. Initial positions of drifters are shown in Figure S1a in Supporting Information S1. Commercial ship tracks and regions of remarkable dynamics (e.g., Gulf Stream) stand out clearly but we checked that the initial distribution of drifters between cyclones and anticyclones was unbiased: the total number of drifters is 5,811, from which 459 were initially in cyclones and 458 in anticyclones (see the following paragraph for the attribution of drifters to eddies).

We first collocated the drifters and eddies in time, considering they were concomitant if their positions are given at times closer than 1 hr. Drifter trajectories are overall coherent with the eddy polarities: drifters spin clockwise (anticlockwise) in the vicinity of anticyclones (cyclones). An animation of drifter trajectories and collocated eddy positions for year 2000 in the North Atlantic Ocean is available in the Supporting Information (Movie S1). We considered that a drifter was inside an eddy if the drifter's distance to the eddy center was smaller than the eddy radius. Since the data set provides eddy areas but not eddy contours, we assumed that eddies were circular and

derived eddy radius from the area. If a drifter appeared to be concomitantly inside two eddies, we considered it belonged to the closest eddy.

2.2. Numerical Framework

In order to carry out a numerical Lagrangian experiment that mimics the drifters spreading, we used the hourly surface velocity and sea surface height (SSH) fields of a numerical simulation of ocean currents in the Atlantic (GIGATL6) that is based on the Coastal and Regional Ocean Community Model (CROCO, developed upon the Regional Oceanic Modeling System, ROMS, Shchepetkin & McWilliams, 2005). GIGATL6 was designed to solve the hydrostatic and primitive equations on a spherical grid encompassing the whole Atlantic Ocean (Greenland to Cape Horn) with a nominal horizontal resolution of 6 km and 50 terrain-following vertical coordinates. The simulation thus resolves mesoscale eddies, with at least 5 grid points to represent the first baroclinic Rossby radius of deformation (R_d) in the region of interest (see Figure 6 in Chelton et al., 1998) and typical mesoscale eddy diameter of 2–3 R_d (Figure 11 in Smith, 2007). The grid bathymetry is from the global SRTM30plus data set (Becker et al., 2009). Initial state and lateral boundary conditions for velocity, SSH, temperature, and salinity are supplied by the Simple Ocean Data Assimilation data set (Carton & Giese, 2008). Atmospheric forcing was supplied at hourly resolution by the Climate Forecast System Reanalysis (Saha et al., 2010). The simulation started in 2004 and our analyses were based on 1 year of outputs in 2009 to ensure that the dynamics were spun up.

Daily SSH outputs from GIGATL6 were fed into the py-eddy-tracker software to detect mesoscale eddies (Mason et al., 2014). In short, py-eddy-tracker sought the outermost closed contours of SSH to identify mesoscale eddies. A series of tests was then applied (shape, size, single maximum of SSH within a closed contour, etc.) to discard features that were likely not eddies. Once the eddies were detected, their closed contours were tracked forward in time. We only retained eddies that lived longer than 7 days to ensure their robustness.

Hourly surface velocity outputs were used to carry out the Lagrangian dispersion experiment using the Pyticles software (Gula et al., 2014). We only used the horizontal velocity field, that is, no vertical advection was performed. Synthetic particles were evenly released on the model grid with a spacing of ≈ 1.3 km between adjacent particles. This spacing was chosen to maximize the number of particles while limiting the computational cost of the experiment. Particles were passively advected by the surface horizontal currents that were bilinearly interpolated in space and linearly interpolated in time at the positions of particles with a 6-min time step.

3. Results

3.1. Drifters Preferentially Cluster in Mesoscale Cyclones

Figures 1a and 1b show the total number of cyclones and anticyclones detected in the Faghmous et al. (2015) daily data set, on a regular $1^\circ \times 1^\circ$ grid (hence, unit is formally “eddy \times day”). As expected, a larger number of eddies is found in boundary currents as compared to the interior of the subtropical gyre and the equatorial band. There is an equipartition of mesoscale cyclones (C) and anticyclones (AC) throughout the domain, with rather patchy binwise relative differences that rarely exceed 50% ($(\#C - \#AC) / \frac{1}{2}(\#C + \#AC)$, Figure 1c). No clear regional pattern emerges and the relative difference over the domain is 1.3% in favor of cyclones.

We also compare the total surface occupied by cyclones and anticyclones (Figures 1d and 1e). Regional differences stand out in the relative difference map (Figure 1f). The most prominent one is the Gulf Stream's extension, whose southern (northern) edge is more covered by cyclones (anticyclones). The overall relative difference remains small, with a total surface occupied by cyclones that is larger by 4.5%.

Figures 1g and 1h show the number of drifters into cyclones and anticyclones on the same grid. In contrast to the relative equipartition of cyclones and anticyclones, there is a clear preference for drifters to be trapped into cyclones, with pronounced regional trends in the southern edge of the Gulf Stream's extension and within the eastern part of the subtropical gyre (Figure 1i). Overall, mesoscale cyclones contain 24% more drifters than their anticyclonic counterparts. Importantly, this asymmetry cannot be explained by a potential asymmetry in the number of, or area covered by, cyclonic vs. anticyclonic eddies. Hence, the trapping asymmetry must be rooted in polarity-dependent kinematics of ocean currents.

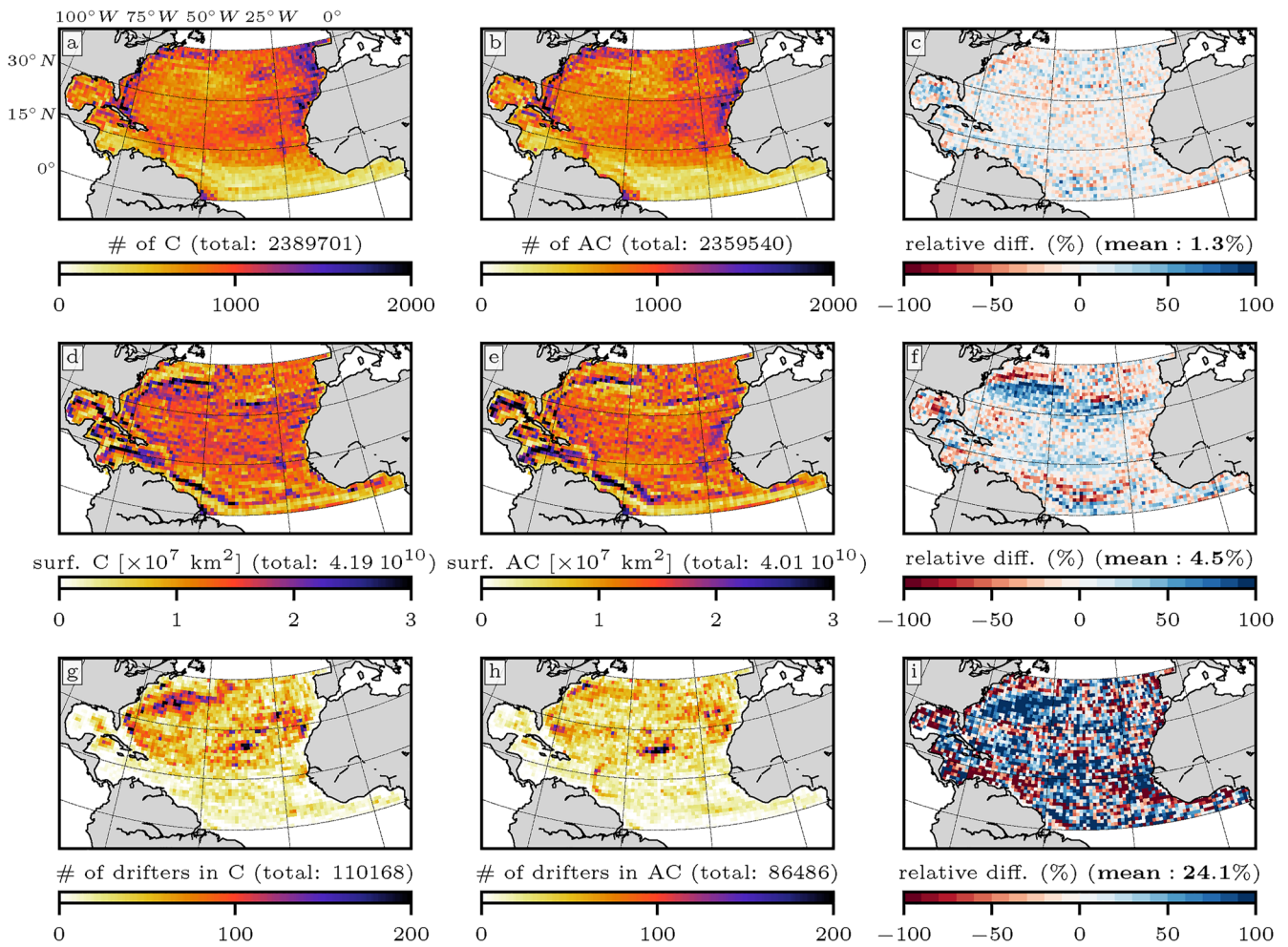


Figure 1. Total number of (a) cyclones, (b) anticyclones, and (c) the relative difference of cyclones vs. anticyclones in $1^\circ \times 1^\circ$ bins. Blue (red) areas are dominated by cyclones (anticyclones). Total surface covered by (d) cyclones, (e) anticyclones, and (f) their relative difference. Total number of (g) drifters in cyclones, (h) in anticyclones, and (i) their relative difference. Blue (red) areas indicate that drifters are preferentially trapped into cyclones (anticyclones). Integrated numbers over the area are given above colorbars.

Complementary to the static maps described above, we examined the number of drifters into cyclones and anticyclones vis-à-vis of the drifters' age (Figure 2). Time series recall that drifters were equally seeded into cyclones and anticyclones (Section 2.1 and Figure 2b). They reveal that the preferred trapping tendency of cyclones builds up within the first ~ 20 days of the drifters' lifecycle and persists over more than 300 days (Figure 2c). Between 20 and 300 days, an average of 20.3% of drifters are found in cyclones vs. 15.4% in anticyclones. After about a year, the total number of drifters has significantly decreased (Figure 2a), and the drifters' coverage of the gyre is scarce (Figures S1c and S1d in Supporting Information S1), hence percentages fluctuate more (Figure 2c). The relative difference between the number of drifters in cyclones and anticyclones reflects the rapidly growing asymmetry, increasing from zero to 15% in 20 days (Figure 2d). Between 20 and 300 days, it fluctuates roughly between 10% and 50%, but overall, within this time period, cyclones contain 27.3% more drifters than anticyclones, consistently with the results that ignored the age of drifters (Figure 1i).

3.2. Synthetic Particles Preferentially Cluster in Mesoscale Cyclonic Fronts and Eddies

To further investigate the reasons behind the trapping asymmetry, we set up a basin-scale Lagrangian dispersion experiment using the model outputs of a 6-km resolution numerical model (Section 2.2). Figure S2 in Supporting Information S1 shows a snapshot of particles' position, surface relative vorticity, and eddy contours. We compute the concentration of particles in eddies for each individual as the number of particles divided by the eddy surface

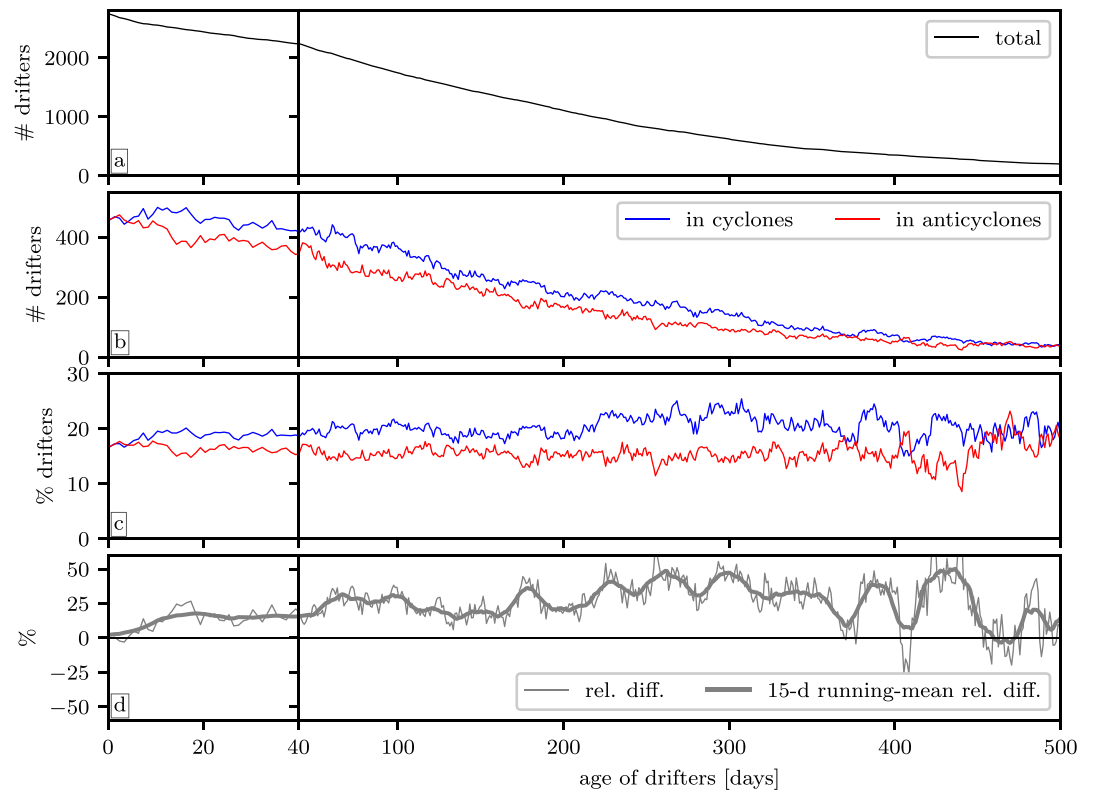


Figure 2. Time series relative to the drifters' age. (a) Total number of drifters in the area; (b) number and (c) percentage of drifters in (blue line) cyclones and (red line) anticyclones; (d) (thin gray line) relative difference of drifters in cyclones vs. in anticyclones and (bold gray line) its 15-day running mean. Positive means that drifters are preferentially trapped into cyclones.

(output by py-eddy-tracker). Then, we derive statistics for each eddy polarity every 5 days. Figure 3a shows time series of the median and quartiles of particle concentration in cyclones and anticyclones. It thus gives an overview of the distribution of particle concentration. The particle concentration in cyclones and anticyclones is strictly equal at the release. The relative difference builds up within the first ≈ 30 days and fluctuates around 20% between 30 and 200 days before increasing and plateauing around 40% (Figure 3b). Reasons for this stepwise evolution remain unclear. However, the modeling results are overall consistent with the observations and confirm that mesoscale cyclones trap more surface buoyant material than anticyclones.

Visual inspection of particles and surface vorticity fields suggests two important points (Movie S2). First, particles cluster preferentially in cyclonic areas, regardless of the type of structures, that is, fronts or eddies. Second, it suggests that the clustering of particles occurs prior to the detection of eddies. Specifically, we routinely observe clusterings of particles in cyclonic fronts before the latter roll up into mesoscale cyclones subsequently detected by the algorithm.

We carried out several diagnostics to confirm those visual impressions. Inspired by Balwada et al. (2021), we examine the mean particle concentration as a function of vertical vorticity ($\zeta = \partial_x v - \partial_y u$, with (u, v) the horizontal velocity in the (x, y) , that is, zonal and meridional, coordinate system) and strain ($\sigma = \sqrt{\sigma_n^2 + \sigma_s^2}$, with $\sigma_n = \partial_x u - \partial_y v$ and $\sigma_s = \partial_x v + \partial_y u$). Figure 4b strongly supports the first observation. Indeed, particle concentration is rather homogeneous ($\approx 1-2 \times 10^{-8} \text{ m}^{-2}$) in most of the vorticity-strain domain but a clear two-to-three times increase in concentration (up to $6 \times 10^{-8} \text{ m}^{-2}$) is found approaching and past the $\sigma = \zeta$ line on the cyclonic side ($\zeta > 0$). This line materializes cyclonic fronts, whereas the area below ($\zeta < \sigma$) is dominated by more materially coherent spinning structures (Balwada et al., 2021).

The second point was tested by identifying particles belonging to an eddy at its first detection and tracking them backward in time to get insights on the trapping scenario. We specifically monitored the flow vorticity

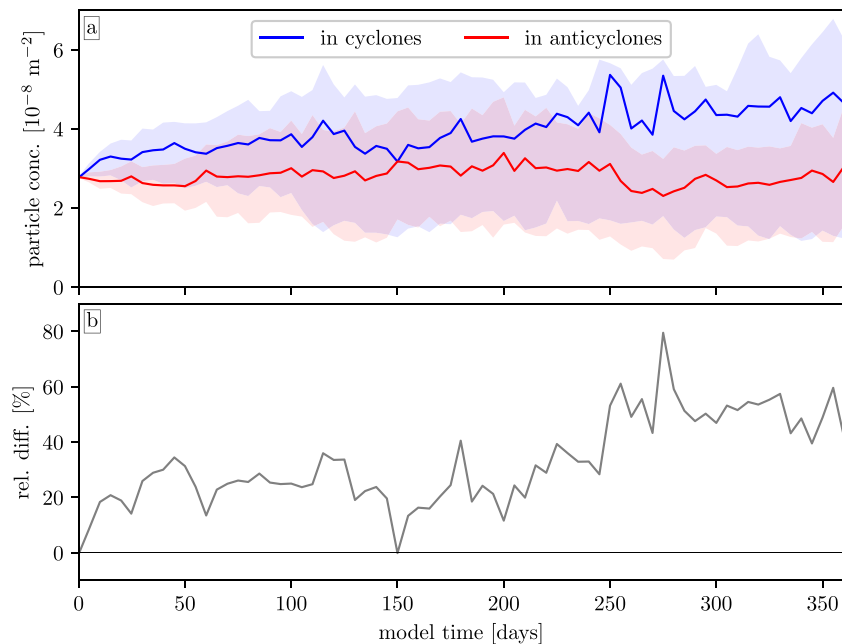


Figure 3. Results from the modeling study. (a) Median and quartiles of the concentration of particles in cyclones and anticyclones and (b) the relative difference computed from the median. Positive means an excess of particles into cyclones.

and divergence ($\delta = \partial_x u + \partial_y v$) interpolated at the particles' position (Figures 4c and 4d). Time series reveal that most particles acquire the polarity of the eddy they are going to get trapped in between 5 and 15 days before the eddy is actually detected. Remarkably, 5 days prior to the eddy detection, more than half of the particles already have the polarity of the eddy they are going to be trapped in (the envelop of quartiles does not cross the zero line, Figure 4c). Note that this tendency is more pronounced for cyclonic flows that feature larger vorticity. Furthermore, δ/f is negative for most particles – they are by definition attracted in convergence zones ($\delta/f < 0$) – and does not show any difference for the cyclonic and anticyclonic cases until ≈ 10 days before the eddy detection (Figure 4d). Around this time, particles that are going to be trapped into cyclones see a negative divergence that is roughly twice as large as the ones that are going to be trapped into anticyclones. This emphasizes the enhanced clustering of particles in cyclonic regions before the actual detection of the mesoscale cyclones they are going to be trapped in.

4. Summary and Discussion

Our study sheds light on the hitherto undocumented asymmetric role of mesoscale eddies to cluster surface buoyant material. Combining surface drifters with a mesoscale eddy database, we demonstrated that cyclones cluster roughly 24% more drifters than anticyclones. A numerical Lagrangian experiment using a mesoscale-resolving model reproduces this asymmetry and helped us to gain insight into the trapping scenario, which is as follows. Statistically, particles are more concentrated in cyclonic regions, including fronts and eddies. For particles that end up being trapped in eddies, a backward tracking indicates that they tend to acquire the eddies' polarity while the eddy is formed, which corresponds to a few days before it is actually detected. This preconditioning is more prominent in cyclonic flows and, added up to the background higher concentration of particles in cyclonic regions, qualitatively explains the asymmetry in particle concentration between mesoscale cyclonic and anticyclonic eddies. Note that we extended the observational analysis to the whole Atlantic Ocean and obtained quantitatively similar results.

At first sight, the clustering asymmetry is unanticipated. Indeed, while in submesoscale-dominated regimes, clustering of material in cyclonic regions is documented and rationalized (Balwada et al., 2021; Berta et al., 2020; D'Asaro et al., 2018; Esposito et al., 2021), such an asymmetry is unexpected at the mesoscale – see the introductory review of literature in Section 1. Our model resolution formally allows an accurate representation of mesoscales but hardly permits submesoscales. This is a posteriori diagnosed through the joint probability density

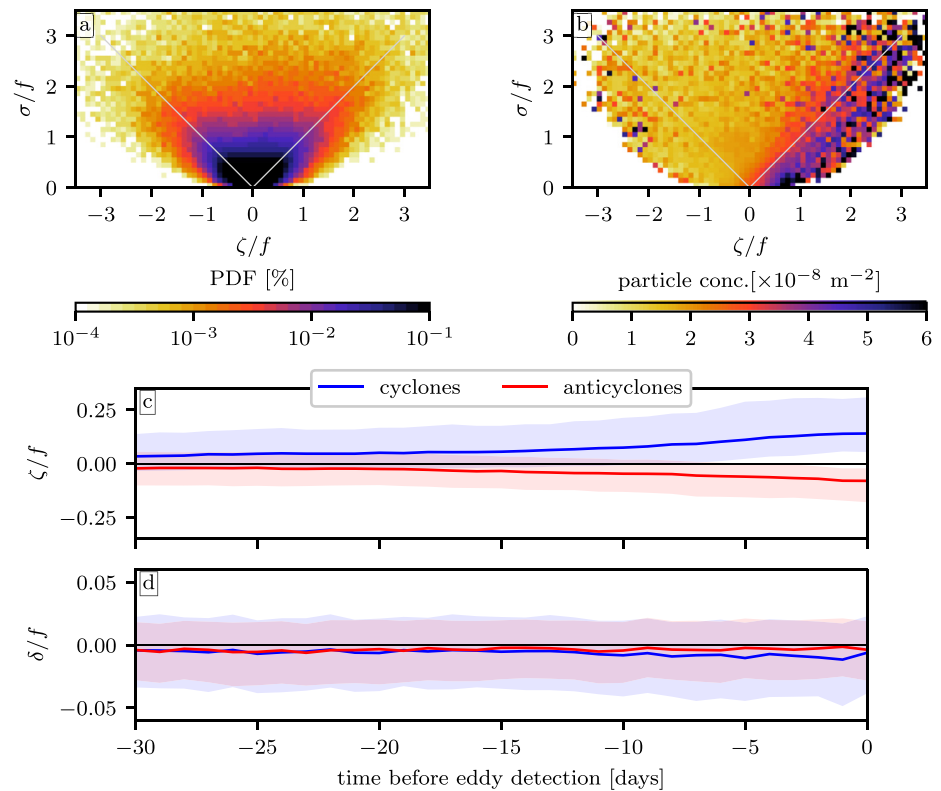


Figure 4. Results from the modeling study. (a) Joint probability density function of relative vorticity ζ/f and strain σ/f , both non-dimensionalized by the local Coriolis frequency. (b) Mean particle concentration per bin in vorticity-strain space (bin width is 0.1). (a and b) are averaged over 16 frames covering the whole domain and evenly spaced in time between 10 and 100 days of simulation. Gray lines represent $\sigma = |\zeta|$. Model (c) vorticity ζ/f and (d) divergence δ/f (median and quartiles), both non-dimensionalized by the local Coriolis frequency, seen by particles before they are trapped into cyclones (blue) and anticyclones (red).

function of vorticity and strain, which is roughly symmetric relative to vorticity, while hinting that ageostrophic currents ($|\zeta/f| > 1$) can develop (Figure 4a). We thus hypothesize that the rare (PDF $< 10^{-2}\%$) ageostrophic frontogenesis that occurs in the model is instrumental at clustering particles in cyclonic fronts and preconditioning the higher concentration in cyclonic eddies. Indeed, the secondary circulation associated with those fronts is key to drive a convergence of material in cyclonic regions (Barkan et al., 2019). Note that this preconditioning is also consistent with the findings of Zhang and Qiu (2018) that showed that ageostrophic motions within mesoscale eddies are intensified at the beginning of their lifecycle.

An examination of the literature on physical-biological-biogeochemical interactions at the mesoscale could not shed us some light over any clear mechanism that could lead to surface clustering. Higher chlorophyll concentrations are consistently found in anticyclones as compared to cyclones, which has to be explained by an enhanced net upward transport of nutrients (observations are reviewed in McGillicuddy, 2016). Several mechanisms are invoked to explain the enhancement of vertical velocities in mesoscale eddies (e.g., Martin & Richards, 2001) but only two have asymmetrical effects in cyclones and anticyclones (eddy pumping and Ekman pumping, reviewed in the introduction, based on McGillicuddy, 2016). Systematically quantifying the importance of those mechanisms is arduous, since eddy pumping intrinsically depends on the generation mechanism, and Ekman pumping depends on wind stress and eddy velocity, both spanning wide ranges of values. Nonetheless, we claim that these two mechanisms do not play a significant role in the asymmetry we observe here. Eddy pumping should lead to a divergence of material in cyclones during their formation, which is opposite to our observations. Ekman pumping could contribute to the increased convergence in cyclones. However, clustering happens prior to the eddy detection and the asymmetry does not change significantly after the eddies are formed, which lead us to consider Ekman pumping as a second-order mechanism to explain the flow convergence in mesoscale cyclones.

Also, note that the literature review of van Sebille et al. (2020) on the physics involved in the dispersion of floating debris only reports one case where plastic concentration was higher in an anticyclone as compared to a neighboring cyclone (Brach et al., 2018). Clearly, this result needs to be statistically tested.

Our study has several limitations. Probably the most important is about the eddy detection and tracking method, regarding both the observational and modeling methods and results. Some recent articles highlighted the inherent limitations of tracking mesoscale eddies through altimetry and/or with SSH-based techniques (e.g., Amores et al., 2018; Stegner et al., 2021). In addition, the classic vision of materially coherent mesoscale eddies has been questioned over the last decade, emphasizing the leakiness of such structures (e.g., Cetina-Heredia et al., 2019; Liu et al., 2019). Furthermore, as the resolution of numerical models and observations increases, emerging submesoscale three-dimensional circulations seem to play a preponderant role in shaping material patterns in the surface layers (e.g., Lévy et al., 2018; Uchida et al., 2019). These questions will be addressed in future work.

Data Availability Statement

The authors downloaded the eddy database from <https://doi.org/10.5061/dryad.gp40h> and the Global Drifter Program data from <https://www.aoml.noaa.gov/phod/gdp/interpolated/data/subset.php>. CROCO ocean model is available at <https://www.croco-ocean.org>. Information about the GIGATL6 simulation can be found at <https://doi.org/10.5281/zenodo.4948523>. The py-eddy-tracker software is available at <https://py-eddy-tracker.readthedocs.io/en/stable/>. The Lagrangian software Pyticles is available at <https://github.com/Mesharou/Pyticles> and has been archived on Zenodo at <https://doi.org/10.5281/zenodo.4973786>.

References

- Abernathy, R., & Haller, G. (2018). Transport by Lagrangian vortices in the Eastern Pacific. *Journal of Physical Oceanography*, 48(3), 667–685. <https://doi.org/10.1175/JPO-D-17-0102.1>
- Amores, A., Jordà, G., Arsoze, T., & Le Sommer, J. (2018). Up to what extent can we characterize ocean eddies using present-day gridded altimetric products? *Journal of Geophysical Research: Oceans*, 123(10), 7220–7236. <https://doi.org/10.1029/2018JC014140>
- Balwada, D., Xiao, Q., Smith, S., Abernathy, R., & Gray, A. R. (2021). Vertical fluxes conditioned on vorticity and strain reveal submesoscale ventilation. *Journal of Physical Oceanography*, 51, 2883–2901. <https://doi.org/10.1175/JPO-D-21-0016.1>
- Barkan, R., Molemaker, M. J., Srinivasan, K., McWilliams, J. C., & D'Asaro, E. A. (2019). The role of horizontal divergence in submesoscale frontogenesis. *Journal of Physical Oceanography*, 49(6), 1593–1618. <https://doi.org/10.1175/JPO-D-18-0162.1>
- Becker, J., Sandwell, D., Smith, W., Braud, J., Binder, B., Depner, J., et al. (2009). Global bathymetry and elevation data at 30 arc seconds resolution: SRTM30_PLUS. *Marine Geodesy*, 32(4), 355–371. <https://doi.org/10.1080/01490410903297766>
- Beron-Vera, F. J., Olascoaga, M. J., & Lumpkin, R. (2016). Inertia-induced accumulation of flotsam in the subtropical gyres. *Geophysical Research Letters*, 43(23), 12–228. <https://doi.org/10.1002/2016GL071443>
- Berta, M., Griffa, A., Haza, A., Horstmann, J., Huntley, H., Ibrahim, R., et al. (2020). Submesoscale kinematic properties in summer and winter surface flows in the Northern Gulf of Mexico. *Journal of Geophysical Research: Oceans*, 125(10), e2020JC016085. <https://doi.org/10.1029/2020JC016085>
- Brach, L., Deixonne, P., Bernard, M.-F., Durand, E., Desjean, M.-C., Perez, E., et al. (2018). Anticyclonic eddies increase accumulation of microplastic in the North Atlantic subtropical gyre. *Marine Pollution Bulletin*, 126, 191–196. <https://doi.org/10.1016/j.marpolbul.2017.10.077>
- Buckingham, C. E., Naveira Garabato, A. C., Thompson, A. F., Brannigan, L., Lazar, A., Marshall, D. P., et al. (2016). Seasonality of submesoscale flows in the ocean surface boundary layer. *Geophysical Research Letters*, 43(5), 2118–2126. <https://doi.org/10.1002/2016GL068009>
- Capet, X., Klein, P., Hua, B. L., Lapeyre, G., & McWilliams, J. C. (2008). Surface kinetic energy transfer in surface quasi-geostrophic flows. *Journal of Fluid Mechanics*, 604, 165–174. <https://doi.org/10.1017/S0022112008001110>
- Carton, J., & Giese, B. (2008). A reanalysis of ocean climate using Simple Ocean Data Assimilation (SODA). *Monthly Weather Review*, 136(8), 2999–3017. <https://doi.org/10.1175/2007MWR1978.1>
- Cetina-Heredia, P., Roughan, M., van Sebille, E., Keating, S., & Brassington, G. B. (2019). Retention and leakage of water by mesoscale eddies in the East Australian Current system. *Journal of Geophysical Research: Oceans*, 124(4), 2485–2500. <https://doi.org/10.1029/2018JC014482>
- Chelton, D. B., DeSzoeke, R. A., Schlax, M. G., El Naggar, K., & Siwertz, N. (1998). Geographical variability of the first baroclinic Rossby radius of deformation. *Journal of Physical Oceanography*, 28(3), 433–460. [https://doi.org/10.1175/1520-0485\(1998\)028<0433:gvotfbs>2.0.co;2](https://doi.org/10.1175/1520-0485(1998)028<0433:gvotfbs>2.0.co;2)
- Chelton, D. B., Schlax, M. G., & Samelson, R. M. (2011). Global observations of nonlinear mesoscale eddies. *Progress in Oceanography*, 91(2), 167–216. <https://doi.org/10.1016/j.pocean.2011.01.002>
- D'Asaro, E. A., Shcherbina, A. Y., Klymak, J. M., Molemaker, J., Novelli, G., Guigand, C. M., et al. (2018). Ocean convergence and the dispersion of flotsam. *Proceedings of the National Academy of Sciences*, 115(6), 1162–1167. <https://doi.org/10.1073/pnas.1718453115>
- Esposito, G., Berta, M., Centurioni, L., Lodise, J., Ozgokmen, T., Poulain, P.-M., et al. (2021). Submesoscale vorticity and divergence in the Alboran Sea: Scale and depth dependence. *Frontiers in Marine Science*, 8, 843. <https://doi.org/10.3389/fmars.2021.678304>
- Faghmous, J. H., Frenger, I., Yao, Y., Warmka, R., Lindell, A., & Kumar, V. (2015). A daily global mesoscale ocean eddy data set from satellite altimetry. *Scientific Data*, 2(1), 1–16. <https://doi.org/10.1038/sdata.2015.28>
- Flierl, G., & McGillicuddy, D. J. (2002). *Mesoscale and submesoscale physical-biological interactions*. In A. Robinson, J. McCarthy, & B. Rothschild (Eds.), (Vol. 12). Wiley.
- Gaube, P., Chelton, D. B., Samelson, R. M., Schlax, M. G., & O'Neill, L. W. (2015). Satellite observations of mesoscale eddy-induced Ekman pumping. *Journal of Physical Oceanography*, 45(1), 104–132. <https://doi.org/10.1175/JPO-D-14-0032.1>
- Grodsky, S. A., Lumpkin, R., & Carton, J. A. (2011). Spurious trends in global surface drifter currents. *Geophysical Research Letters*, 38(10). <https://doi.org/10.1029/2011GL047393>

Acknowledgments

J.G. gratefully acknowledges support from the French National Agency for Research (ANR) through the project DEEPER (ANR-19-CE01-0002-01). J.G. acknowledges PRACE and GENCI for awarding access to HPC resources Joliot-Curie Rome and SKL from GENCI-TGCC (Grants 2020-A0090112051, 2019gch0401 and PRACE project 2018194735) and HPC facilities DATARMOR of “Pôle de Calcul Intensif pour la Mer” at Ifremer (Brest, France). The authors thank Gildas Cambon and Sébastien Theetten for their contribution in the development of the realistic numerical simulation GIGATL6.

- Gula, J., Molemaker, M. J., & McWilliams, J. C. (2014). Submesoscale cold filaments in the Gulf Stream. *Journal of Physical Oceanography*, 44(10), 2617–2643. <https://doi.org/10.1175/JPO-D-14-0029.1>
- Lévy, M., Franks, P. J., & Smith, K. S. (2018). The role of submesoscale currents in structuring marine ecosystems. *Nature Communications*, 9(1), 4758. <https://doi.org/10.1038/s41467-018-07059-3>
- Liu, T., Abernathy, R., Sinha, A., & Chen, D. (2019). Quantifying Eulerian eddy leakiness in an idealized model. *Journal of Geophysical Research: Oceans*, 124(12), 8869–8886. <https://doi.org/10.1029/2019JC015576>
- Lumpkin, R., & Pazos, M. (2007). *Measuring surface currents with Surface Velocity Program drifters: The instrument, its data, and some recent results*. In A. Griffa, A. Kirwan Jr., A. J. Mariano, T. Özgökmen, & H. T. Rossby (Eds.), Cambridge University Press.
- Martin, A. P., & Richards, K. J. (2001). Mechanisms for vertical nutrient transport within a North Atlantic mesoscale eddy. *Deep-Sea Research Part II*, 48(4–5), 757–773. [https://doi.org/10.1016/S0967-0645\(00\)00096-5](https://doi.org/10.1016/S0967-0645(00)00096-5)
- Mason, E., Pascual, A., & McWilliams, J. C. (2014). A new sea surface height-based code for oceanic mesoscale eddy tracking. *Journal of Atmospheric and Oceanic Technology*, 31(5), 1181–1188. <https://doi.org/10.1175/JTECH-D-14-00019.1>
- McGillicuddy, D. J., Jr. (2016). Mechanisms of physical-biological-biogeochemical interaction at the oceanic mesoscale. *Annual Review of Marine Science*, 8, 125–159. <https://doi.org/10.1146/annurev-marine-010814-015606>
- McWilliams, J. C. (2008). The nature and consequences of oceanic eddies. *Ocean modeling in an eddying regime*, 177, 5–15. <https://doi.org/10.1029/177GM03>
- Niiler, P. (2001). The world ocean surface circulation. *International Geophysics*, 77, 193–204. [https://doi.org/10.1016/S0074-6142\(01\)80119-4](https://doi.org/10.1016/S0074-6142(01)80119-4)
- Penven, P., Halo, I., Pous, S., & Marié, L. (2014). Cyclogeostrophic balance in the Mozambique Channel. *Journal of Geophysical Research: Oceans*, 119(2), 1054–1067. <https://doi.org/10.1002/2013JC009528>
- Polvani, L. M., McWilliams, J. C., Spall, M. A., & Ford, R. (1994). The coherent structures of shallow-water turbulence: Deformation-radius effects, cyclone/anticyclone asymmetry, and gravity-wave generation. *Chaos*, 4(2), 177–186. <https://doi.org/10.1063/1.166002>
- Poulain, P.-M., Gerin, R., Mauri, E., & Pennel, R. (2009). Wind effects on drogued and undrogued drifters in the eastern Mediterranean. *Journal of Atmospheric and Oceanic Technology*, 26(6), 1144–1156. <https://doi.org/10.1175/2008JTECH0618.1>
- Roulet, G., & Klein, P. (2010). Cyclone-anticyclone asymmetry in geophysical turbulence. *Physical Review Letters*, 104(21), 218501. <https://doi.org/10.1103/PhysRevLett.104.218501>
- Rudnick, D. L. (2001). On the skewness of vorticity in the upper ocean. *Geophysical Research Letters*, 28(10), 2045–2048. <https://doi.org/10.1029/2000GL012265>
- Saha, S., Moorthi, S., Pan, H.-L., Wu, X., Wang, J., Nadiga, S., et al. (2010). The NCEP climate forecast system reanalysis. *Bulletin of the American Meteorological Society*, 91(8), 1015–1058. <https://doi.org/10.1175/2010BAMS3001.1>
- Shchepetkin, A., & McWilliams, J. (2005). The regional oceanic modeling system (ROMS): A split-explicit, free-surface, topography-following-coordinate oceanic model. *Ocean Modeling*, 9(4), 347–404. <https://doi.org/10.1016/j.ocemod.2004.08.002>
- Shcherbina, A. Y., D'Asaro, E. A., Lee, C. M., Klymak, J. M., Molemaker, M. J., et al. (2013). Statistics of vertical vorticity, divergence, and strain in a developed submesoscale turbulence field. *Geophysical Research Letters*, 40(17), 4706–4711. <https://doi.org/10.1002/grl.50919>
- Smith, K. S. (2007). The geography of linear baroclinic instability in Earth's oceans. *Journal of Marine Research*, 65(5), 655–683. <https://doi.org/10.1357/002224007783649484>
- Stegner, A., Le Vu, B., Dumas, F., Ghannami, M. A., Nicolle, A., Durand, C., et al. (2021). Cyclone-anticyclone asymmetry of eddy detection on gridded altimetry product in the Mediterranean Sea. *Journal of Geophysical Research: Oceans*, 126(9), e2021JC017475. <https://doi.org/10.1029/2021JC017475>
- Uchida, T., Balwada, D., Abernathy, R., McKinley, G., Smith, S., & Levy, M. (2019). The contribution of submesoscale over mesoscale eddy iron transport in the open Southern Ocean. *Journal of Advances in Modeling Earth Systems*, 11(12), 3934–3958. <https://doi.org/10.1029/2019MS001805>
- Vallis, G. K. (2006). *Atmospheric and oceanic fluid dynamics: Fundamentals and large-scale circulation*. Cambridge University Press.
- van Sebille, E., Aliani, S., Law, K. L., Maximenko, N., Alsina, J. M., & Bagaev, A. (2020). The physical oceanography of the transport of floating marine debris. *Environmental Research Letters*, 15(2), 023003. <https://doi.org/10.1088/1748-9326/ab6d7d>
- Zhang, Z., & Qiu, B. (2018). Evolution of submesoscale ageostrophic motions through the life cycle of oceanic mesoscale eddies. *Geophysical Research Letters*, 45(21), 11–847. <https://doi.org/10.1029/2018GL080399>
- Zhang, Z., Wang, W., & Qiu, B. (2014). Oceanic mass transport by mesoscale eddies. *Science*, 345(6194), 322–324. <https://doi.org/10.1126/science.1252418>